www.czasopisma.pan.pl PAN POLSKA AKADEMIA NAUK www.journals.pan.pl

Arch. Metall. Mater. **67** (2022), 2, 535-540

DOI: https://doi.org/10.24425/amm.2022.137787

A.C. BERBECARU[1], G. COMAN[1], S. CIUCĂ[1], I.A. GHERGHESCU[1*], M.G. SOHACIU[1], C. GRĂDINARU[1], C. PREDESCU[1*]

RESEARCH ON THE DEGRADATION PROCESS OF RAILWAY RAILS DUE TO LIFESPAN EXCEEDING

The paper presents the impact of exceeding the railway rails lifespan which usually causes a railway structural failure, thus an accident. The research highlights the rails's high degradation, especially on the running area, consisting in 60-70% weight loss by advanced wear of the rail, followed by fatigue fracture caused by alternating cyclic stresses that initiates the crack and also by tensile stresses resulting in the crack growth. The chemical composition, structural and mechanical properties were analyzed in order to establish the causes that led to the railway rails rupture.

Keywords: Degradation; Advanced wear; Fatigue fracture; Railway rails lifespan

1. Introduction

Rail transport is one of the most important means of transport in terms of cost, safety, time and reliability, being one of the less polluting methods of transport. Rail transport is accessible for high volume loads and does not raise traffic problems, the waiting time being considered minimal. In recent decades, railway infrastructure has been widely expanded in urban and rural areas. Given the importance of this type of transport, the maintenance of the track (line rails) in good condition and safe operating along the service life are a priority. Also, the prediction of railway degradation is very important in order to optimize and reduce the railways maintenance and operating costs [1,2].

Of great importance also is maintenance planning, through a wide range of management systems of transport engineering assets, optimization planning and decision making in order to avoid accidents due to poor maintenance of the track system [3]. The line rails are highly strained hence being made of very high quality steel. Many decades are needed to improve the quality of the material. Minor steel defects that may not be a problem in other applications can lead to broken rails and dangerous derailment when used on rail tracks.

2. Materials and methods

The present research aimed to determine the causes that led to the degradation of the railway tracks as a result of exceeding their lifespan, which led to the occurrence of a railway accident. The investigated material was a line rail coupon in the breaking area that showed numerous defects of the contact surface. Figure 1 shows the aspect of this tested and analyzed sample.

Fig. 1. Coupon aspect in the fracture zone

The following investigation tests were performed:

– determination of the chemical composition by optical emission spectrometry, using the LECO GDS 500A spectrometer;

[1] POLITEHNICA UNIVERSITY OF BUCHAREST, FACULTY OF MATERIALS SCIENCE AND ENGINEERING, 313 SPLAIUL INDEPENDENȚEI, 060042 BUCHAREST, ROMANIA

* Corresponding author: gherghescu_ioana@yahoo.com; ioana.gherghescu@upb.ro

– macroscopic analysis of the affected surfaces;
– Brinell hardness tests were performed on universal static hardness testing machine BUEHLER-WILSON, REICHERTER UH 250;
– optical microscopy metallographic analyses were performed on an OLYMPUS BX 51 M microscope;
– tensile tests were performed using the 250 kN, INSTRON MODEL 8802 universal tensile testing machine.
– the impact test was performed using the INSTRON 450 MPX V2-J1 motorized pendulum impact testing system accessorized with Charpy hammer.

3. Results and discussions

The results obtained from the analyzes and investigations performed are presented as follows.

3.1. Sample chemical composition analysis

The line rail sample chemical composition determined by optical emission spectrometry is shown in Table 1.

From the compositional data, the material falls into the grade R260, frequently used in the production of "VIGNOLE" type line rails.

3.2. Macroscopic analysis of the fractured surfaces

Figure 2 shows the breaking areas and surfaces of the line rail that were macroscopically examined.

The macroscopic analysis of fracture surfaces suggests a classic type of rolling contact fatigue fracture under alternating cycles.

Fatigue is the progressive and localized structural damage that occurs when a material is subjected to cyclic loading. The nominal maximum stress values are less than the ultimate tensile stress limit, and may be below the yield stress limit of the material.

Fracture occurs by a three step process involving:

1. nucleation of a crack (initiation): the nucleation sides are near the surface and are represented by surface defects: scratches, sharp corners due to the poor design or manufacture, inclusions or dislocation concentrations;
2. slow cyclic propagation of the crack (fatigue crack propagation);
3. catastrophic failure of the metal (fast fracture).

One has to mention that cyclic stress initiates the crack but tensile stress is also involved in the crack growth, up to the final fast fracture.

Thus, in the upper part of the line rail (rail head), several microcracks appear which, under stress, are propagating slowly and intermittently. In that region, the appearance of the surfaces separated by the crack has a smooth character, which shows that the fracture was advancing through the ductile mechanism. Once the effective section has been exceeded, the rupture progresses rapidly, according to the fragile mechanism. The advancing direction is uncontrolled, exhibiting a jag or spaced faults feature, quickly traversing the rail web and ending in the rail base. The feature in these areas is grained, rough, specific to fragile rapid rupture. Considering our line rail coupon and evaluating the surface quality of the rail head in longitudinal plan but also from a side view, its advanced wear is very clearly highlighted.

Fatigue fractures may be generated as a consequence of mechanical loading, of a thermal loading or may be a result of the combination of both mechanical and thermal loadings [4].

But several other defects are induced by a crack initiation and a propagation phenomenon, not necessarily a fatigue fracture.

TABLE 1

Line rail sample chemical composition values

Chemical element / Sample vs. reference material	C %	Mn %	Si %	S %	P %	Cu %	Cr %	Ni %	Ti %
Sample* (R260 – like)	0.821	0.971	0.257	0.026	0.013	0.011	0.019	0.015	0.020
R260 (SR EN 13674-1)	0.60-0.82	0.65-1.25	0.13-0.60	0.008-0.03	max. 0.030	0.15	max. 0.15	0.1	0.025

* Part of the studied line rail piece.

Fig. 2. Aspect of macroscopically analyzed areas and fracture surfaces

The crack initiation and propagation processes resulting from a mechanical loading have been widely studied [5-9]. Thermally damaged surface layers, called white etching layers (WELs), also contribute to crack initiation [10-13]. Cracks nucleating in or close to WELs can develop into so-called squats and studs on the rail head [4], leading to delaminations, which are numerous on our studied coupon.

There are many areas where the metallic material shows cracks, damaged surface layers and severe delaminations. From the side view one may see the specific gauge corner (fillet) zones being very asymmetrical, with different fillet radii and uneven opening angles that suggest advanced wear.

3.3. Vickers hardness tests

Vickers hardness tests were chosen in order to establish the hardness distribution in the sample's cross section. Figure 3 shows the hardness distribution diagram in the line rail cross-section.

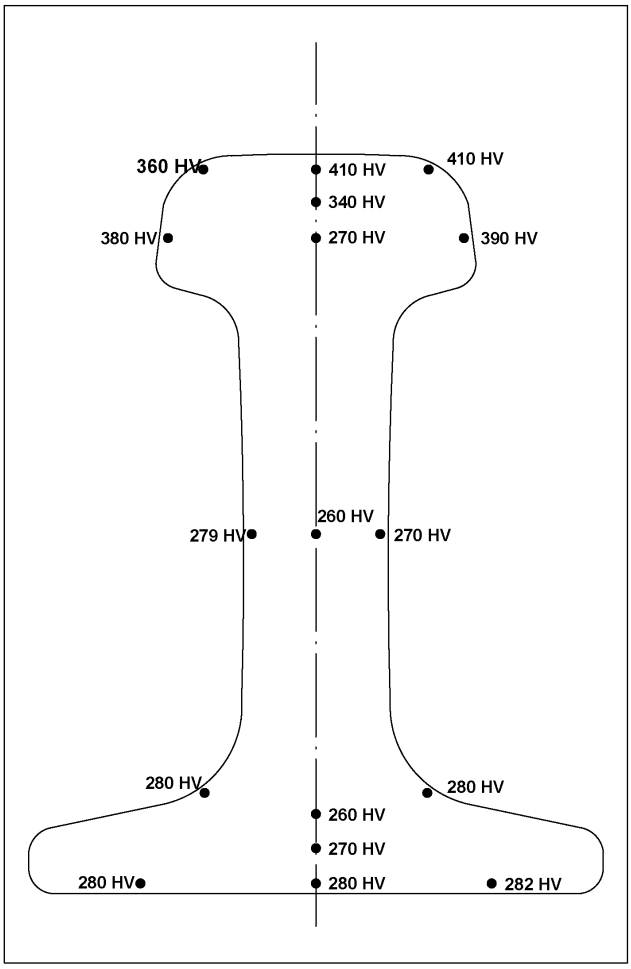

Fig. 3. Vickers hardness values distribution on the line rail sample cross-section

Table 2 shows Vickers hardness values tested on the top of the rail head. Three tests were performed.

TABLE 2

Vickers hardness values tested on the top of the rail head

Sample /Test	Vickers hardness HV1
	Steel grade R260 – like
1	360
2	410
3	410
Average value	394

The hardness distribution on the line rail profile in the three areas: rail head, rail web and rail base highlights the following:

– RAIL HEAD – in the upper part one can find higher values (360-410 HV) that lower down to a stable value of 270 HV in its core zone;
– RAIL WEB – the average hardness values are of approximately 270 HV;
– RAIL BASE – the average hardness values are of approximately 280 HV; these average values of approximately 270 HV are characteristic for the equilibrium structure of a slightly hypereutectoid, light alloyed steel, such as the line rail that is under investigation.

The hardness values recorded on the top of the rail head and on the gauge corner and symmetrical zone (fillet zones) suggest the modification of the structure over time by surface hardening phenomena, meaning *a strain hardening,* phenomenon consisting in a hardening under load. It is also known as *work (cold) hardening:* in a steel structure submitted to a load, the ferrite flattens and the cementite lamellae fragment, becoming preferentially oriented along with the ferrite crystals (or lamellae), respectively perpendicular to the load direction. It is the stress type the line rails are usually submitted to in service.

3.4. Metallographic analysis

Metallographic investigations were performed by optical microscopy as follows:

A) on unetched samples – for the evaluation of the material inclusions;
B) on etched samples – to highlight the metallographic structure of the steel. The etching was performed with the specific ferrous alloys chemical reagent, Nital 2%. Samples were previously prepared according to standard procedures. Thus, they were cut and, using a coolant in order to avoid local overheating that would modify the structure, they were embedded in resin, ground and polished.

Samples were incorporated in two ways – in cross section and in longitudinal section.

A) Unetched samples

The highlighted inclusion state is considered to be a correct one, according to the steel chemical composition determined by optical emission spectrometry. The analysis was performed both in longitudinal section and in cross section at ×100 magnification, according to the specialized standard. Very relevant are the examinations performed in longitudinal section. Thus, one

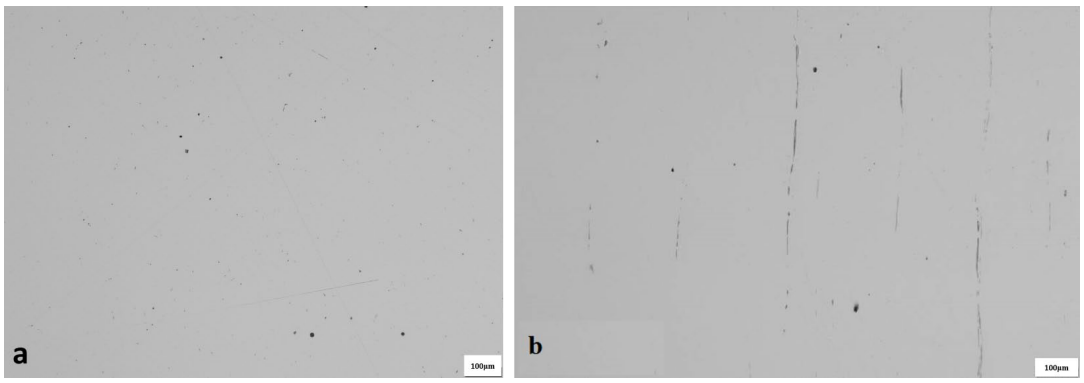

Fig. 4. Optical micrographs of the unetched samples: a) cross-section, b) longitudinal section, 100×

can observe either dispersed, crushed inclusions with angular edges, considered to be alumino-silicates resulted from specific deoxidation reactions taking place along the smelting process, or continuous, elongated inclusions identified as plastic inclusions of MnS, also forming on smelting from desulfurization reactions. All inclusions, without exception, show a preferential orientation being aligned along the hot rolling stress direction, the deformation process being part of the line rails manufacture technology.

B) Etched samples

The samples were analyzed by optical microscopy in order to determine their microstructural features. Samples from the line rail head, web and base were cut and prepared for analysis. The images in the following figures show the optical micrographs, performed at magnifications of 100× and 500×, respectively.

In Figure 5(a), the microstructure recorded in the superficial area a very thin layer on the line rail head.

Figure 5(b) reveals better the superficial layer, having a depth of 20-40 µm and a rather fine needle – like feature, that is, in fact, deformed pearlite. Consequently to a very long time load application, perpendicular to the top of the rail head, the ferrite lamellae flatten, the cementite lamellae shatter, becoming preferentially oriented along the thinned ferrite lamellae, also perpendicular to the load application direction. The structure

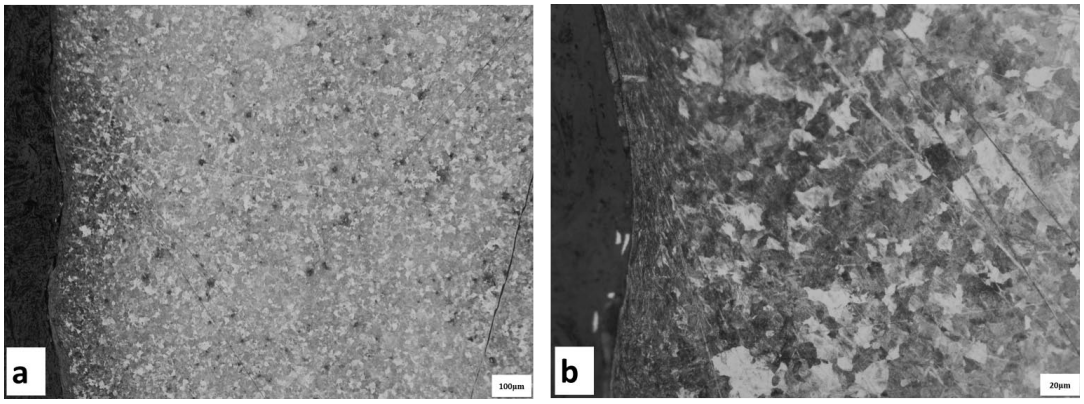

Fig. 5. Optical micrographs of the line rail head, reagent Nital 2%, a) 100×, b) 500×

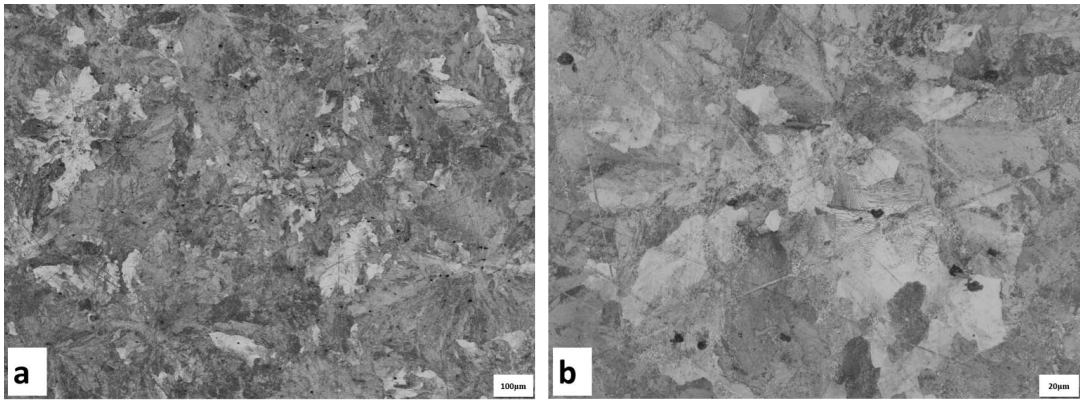

Fig. 6. Optical micrographs of the line rail web, reagent Nital 2%, a) 100×, b) 500×

evolves towards the rail web and stabilizes when reaching the core zone, being mainly formed of lamellar perlite that corresponds to the initial structure. Some similar gradient structures were reported in other studies [14].

One may also notice in Figure 5 an irregular profile of the rail head exterior side and fillet, suggestive of an advanced wear process that took place in a long operating time of the line rail.

The structures corresponding to the rail web and rail base zones (Fig. 6 and Fig. 7) are lamellar perlite equilibrium structures, expected to be found in a steel with this chemical composition.

These HBW values are equivalent to 270-310 HV, thus the hardness values recorded fall into the norm interval for R260 steel grade.

Hence the steel submitted to the investigation has the same mechanical characteristics values as the R260 steel which is the widely used for manufacturing line rails nowadays.

The only difference reported is that of a higher Vickers hardness value (400 HV) on the top of the head rail, resulted as a consequence of the strain hardening phenomenon.

Mechanical tests showed that the line rail steel being under investigation was correctly chosen.

3.5. Mechanical tests

Figure 8 shows the stress-strain curve obtained by tensile testing as well as values of ultimate tensile strength (1014 MPa), elongation at break (A = 13%), striction (Z = 19%).

Besides these values, one can easily read on the diagram that the yield strength is approximately 500 MPa.

According to the SR EN 13674-1 norm, the R260 steel grade must have the following mechanical characteristics values: R_m = min. 880 MPa; A = min 10%; HBW = 260-300, on the longitudinal axis.

3.6. Impact toughness test

Impact toughness indicates toughness of a material using the value of impact energy absorbed by the material during fracturing under impact.

Material impact toughness can be measured by various types of test such as the Charpy V-notch impact test which was chosen for the present study. The test was performed at 20°C. The Charpy specimen was sectioned from the rail head, transversely on the line rail running direction. The test result is shown in Table 3.

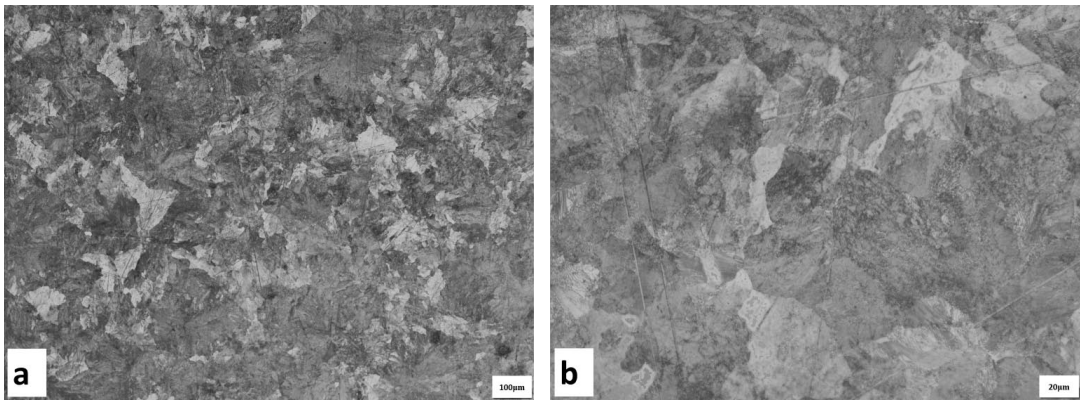

Fig. 7. Optical micrographs of the line rail base, reagent Nital 2%, a) 100×, b) 500×

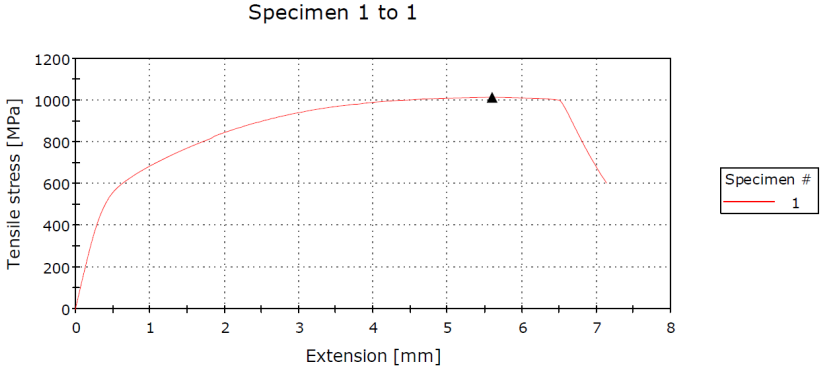

	A %	Z %	Tensile stress at Maximum Load [MPa]	Load at Break (Standard) [kN]
1	12.96	19.00	1014.28	79.24

Fig. 8. Stress-strain curve obtained by tensile testing, values of yield strength and ultimate tensile strength, elongation at break (A%), striction (Z%)

TABLE 3

Impact toughness values

Sample R260 – like	Impact toughness KV, absorbed energy [J]
1	3.46
2	3.48
3	3.43
Average value	3.46

As one can see, the absorbed energy at impact at 20°C is somewhat smaller as compared to that of other pearlitic steels [15]. In the cited reference, at 20°C the absorbed energy value is 5 J, while the value of our tested steel is by 30% smaller.The phenomenon is explained by the existence of microstructural cracks due to an exeedingly long period of time in service.

4. Conclusions

According to the chemical composition, the material falls into the category of a steel grade R260, used in the manufacture of line rails; macroscopic analysis showed an advanced rails wear, especially in the area of maximum cyclic stress (rail head), which led to the fatigue rupture failure.

The hardness values are in accordance with the chemical composition, but also with the structure modified externally by a surface treatment, of mechanical type known as strain hardening.

The metallographic analysis highlighted for all the analyzed samples some structurally correct microstructures, specific to the steel grade used in the line rails manufacture. When examining the fillet zone one may see the superficial area exhibiting a very advanced wear with pronounced unevenness.

Mechanical tests showed that the steel grade used in the line rails fabrication was correctly chosen. Mechanical characteristics fall into the standardized values, excepting the impact toughness. The absorbed energy shows a smaller value (3,43 vs. 5 J), suggesting the existence of structural microcracks.

All corroborated data resulting from the analyses performed on the line rails samples highlight their advanced wear, especially in the area of maximum cyclic stress (rail head), which generates the classic phenomenon of fatigue rupture. This is due to the use of the line rail well above its safe operating limit.

REFERENCES

[1] M.Ph. Papaelias, C. Roberts, C.L. Davis, A review on non-destructive evaluation of rails: state-of-the-art and future developments, J. Rail Rapid Transit, 367-384 (2008).

[2] H. Schwarz, Improving the sustainability of transport – The rail sector as a case study, International Union of Railways Report, New York, 2011

[3] A. Ekberg, B. Åkesson, E. Kabo, Wheel/rail rolling contact fatigue – Probe, predict, prevent, Wear **314** (1-2), 2-12 (2014).

[4] Casey Jessop, Damage and defects in railway materials: Influence of mechanical and thermal damage on crack initiation and propagation, PhD Thesis, Department of Industrial and Materials Science, Chalmers University of Technology, Gothenburg, Sweden, 2019.

[5] M. Steenbergen, R. Dollevoet, On the mechanism of squat formation on train rails – Part I: Origination, Int. J. Fatigue **47**, 361-372 (2013).

[6] M. Steenbergen, R. Dollevoet, On the mechanism of squat formation on train rails – Part II: Growth, Int. J. Fatigue **47**, 373-381 (2013).

[7] S.L. Grassie, D.I. Fletcher, E.A. Gallardo-Hernandez, P. Summers, 'Squats' and 'studs' in rails: similarities and differences, Proc. Inst. Mech. Eng. Part F J. Rail Rapid Transit **226** (3), 243-256 (2011).

[8] J.E. Garnham, J.H. Beynon, The early detection of rolling-sliding contact fatigue cracks, Wear **144** (1-2), 103-116 (1991).

[9] S.L. Grassie, Squats and squat-type defects in rails: the understanding to date, J. Rail Rapid Transit **226**, 235-242 (2011).

[10] C. Bernsteiner, G. Müller, A. Meierhofer, K. Six, D. Künstner, P. Dietmaier, Development of white etching layers on rails : simulations and experiments **367**, 116-122 (2016).

[11] W. Österle Rooch, H., Pyzalla, A., Wang, L., Investigation of white etching layers on rails by optical microscopy, electron microscopy, X-ray and synchotron X-ray diffraction, Mater. Sci. Eng. A **303**, 150-157 (2001).

[12] R.I. Carroll, J.H. Beynon, Rolling contact fatigue of white etching layer: Part 1 Crack morphology, Wear **262**, 1253-1266 (2007).

[13] S. Pal, W. Daniel, M. Farjoo, Early stages of rail squat formation and the role of a white etching layer, Int. J. Fatigue **52**, 144-156 (2013).

[14] A. Yuriev, V. Kormyshev, V. Gromov, Y. Ivanov, A. Semin, Formation of gradient structure in rails at long-term operation, Mat. Res. **23** (6), 1-6 (2020).

[15] http://www.phase-trans.msm.cam.ac.uk/parliament.html, Innovation in Rail Steel, Mr. J.K. Yates Manager, Product Development and Technical Support British Steel Track Products.